Contact Angle of Glycerol Nanodroplets Under van der Waals Force

ARTICLE *in* THE JOURNAL OF PHYSICAL CHEMISTRY C · SEPTEMBER 2009

Impact Factor: 4.77 · DOI: 10.1021/jp905350p

Contact Angle of Glycerol Nanodroplets Under van der Waals Force

Jun Ma,[†,§] Guangyin Jing,[†,⊥] Shiyi Chen,*[,‡,∥] and Dapeng Yu*[,†]

State Key Laboratory for Mesoscopic Physics, Department of Physics, and State Key Laboratory for Turbulence and Complex Systems, College of Engineering, Peking University, Beijing 100871, People's Republic of China, Department of Materials Science and Engineering and Department of Mechanical Engineering, The Johns Hopkins University, Baltimore, Maryland 21218, and Physico-Chimie des Polymeres et des Milieux Disperses, UMR CNRS 7615, ESPCI, 10 rue Vauquelin, F-75231 Paris Cedex 05, France

Received: June 7, 2009; Revised Manuscript Received: July 30, 2009

We have studied the contact angle of glycerol nanodroplets on a partial wetting substrate using the tapping mode of an atomic force microscope. Our experiment shows strong contact angle hysteresis of nanodroplets (radius <100 nm) on mica substrate with atomic-level roughness. The theoretical analysis reveals and our experiment confirms that the van der Waals (vdW) force becomes a critical factor for the mechanical balance of droplets as the drop size reduces to nanometers. The vdW force introduces a dispersion force that significantly lowers the force threshold for producing contact angle hysteresis.

1. Introduction

Wetting is an important physical phenomenon that happens ubiquitously in nature.[1,2] In general there are two kinds of wetting:[2] total wetting, for which the liquid spreads completely to form a film on substrate, and partial wetting, for which the liquid forms a spherical cap (droplet) on substrate. In the mechanical equilibrium of partial wetting, the cosine of the contact angle θ of a droplet on substrate is given by the relation of surface tensions in Young's equation,[2−5] which has been widely used for macroscopic droplets. However, when the droplet size reduces to microscale, the line tension becomes important in the force balance and Young's formula should be modified. The modified Young's equation shows that cos θ is a linear function of $1/r$ (r is the radius of the droplet).[6−9] Pompe and Herminghaus studied nanoscale liquid topographies of a micrometer sized liquid droplet deposited on the hydrophobic and hydrophilic stripes of the substrate and found a linear dependence of cos θ on $1/r$.[9] Checco et al. have found a nonlinear dependence of cos θ on $1/r$ for the alkane droplets with radii of several hundreds of nanometers.[10] Recently, there have been further experimental and theoretical studies on nanoscale liquid. Barberis and Capurro studied the equilibrium shape of nanodroplets by experiments and developed a continuum mechanics model, indicating contact angle depending on the drop size.[11] LV et al. showed theoretically that nonlinear effects of line tension lead to multiple equilibrium shapes of nanodroplets.[12]

As the thickness of the liquid film reduces to nanometers, the van der Waals (vdW) force produces a pressure in the film, or so-called disjoining pressure,[2,13] which is a key factor in the mechanical equilibrium of the film.[2] Analogous to thin film, as the height of the droplet further decreases to nanometers, the vdW force also plays an important role in the force balance. At 50% relative humidity, Xu and Salmeron[14] studied the condensation of glycerol on mica and indicated that the contact angle of droplets increases with the height of droplets increasing up to ∼20 nm. However, when the height is more than 20 nm, the contact angle remains constant. They attributed this phenomenon to the effect of disjoining pressure. de Gennes[2] and Brochard-Wyart et al.[15] presented a theoretical analysis for droplets under vdW forces. However, little experimental work on the nanodroplet with a radius less than 100 nanometers is available. Thus, the role of the vdW force on the contact angle of the nanodroplet is unclear. The atomic force microscope (AFM) technique has become more mature and powerful in recent years, it becomes possible to design delicate experiments to measure the contact angle of nanodroplets (r < 100 nm) precisely. The major objective of this paper is to report experimental studies of contact angle of nanodroplets under the effect of the vdW force.

2. Experimental Section

To produce nanodropets, a pure glycerol droplet of millimeter size was placed on a muscovite mica (Veeco Instruments Inc., Santa Barbara, CA) substrate and blown by a dry nitrogen gas jet. Previous studies show that the nanoscale liquid topographies can be measured by AFM of tapping[9] and noncontact modes,[10] and scanning polarization force microscopy (SPFM).[11,14] We adopted the AFM tapping mode to image nanodroplets. A commercial AFM (sp3800 + spa300; Seiko inc., Japan) equipped with a tapping-mode probe holder was employed. For high-resolution imaging, the AFM unit was placed on a vibration-isolated gas bath. The sample was enclosed in the AFM chamber of dry purified nitrogen gas (N_2) to avoid forming the water bridge in air between the tip and droplet surface. A 120 μm long silicon cantilever has a calibrated force constant of about 17 N/m (Pointprobe sensor, Nanosensors, Germany). The drive frequency of the cantilever is 125 kHz as determined by a Q curve test (Q = 360) embedded in the probe station, which is close to the natural resonance frequency of the cantilever in nitrogen. To achieve an efficient coupling between the drive voltage and the cantilever amplitude response, the vibration voltage was set at 0.15 V to make the amplitude

* Corresponding author. Email: yudp@pku.edu.cn, syc@jhu.edu.
† State Key Laboratory for Mesoscopic Physics, Department of Physics, Peking University.
‡ State Key Laboratory for Turbulence and Complex Systems, College of Engineering, Peking University.
§ Department of Materials Science and Engineering, The Johns Hopkins University.
∥ Department of Mechanical Engineering, The Johns Hopkins University.
⊥ Physico-Chimie des Polymeres et des Milieux Disperses.

10.1021/jp905350p CCC: $40.75
Published on Web 08/17/2009

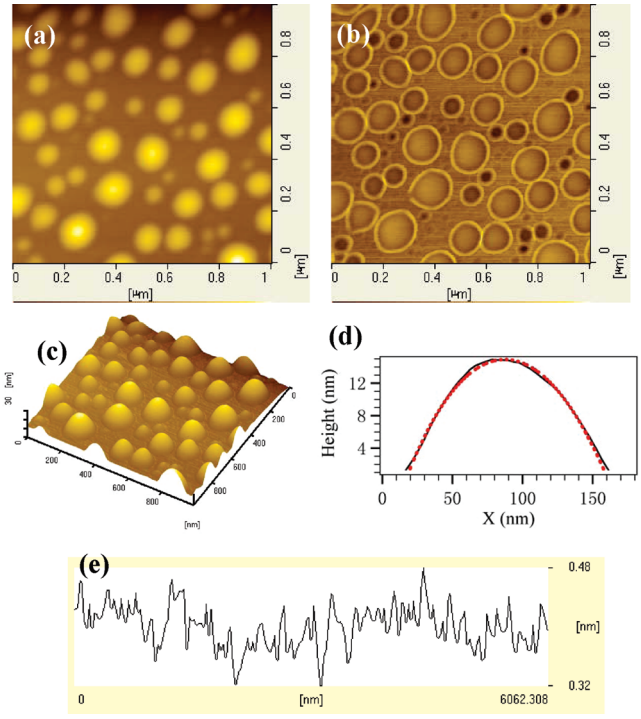

Figure 1. Nanodroplet profiles measured by AFM. (a) Topography image revealing the circular shape of nanodroplets on the mica substrate. (b) Phase image of the nanodroplets in panel a. (c) Three-dimensional image of sphere-cap morphology of the nanodroplets in panel a. (d) Cross section of nanodroplet (black line) showing a sphere-cap profile (fitting sphere (red dots)). *X*, radial direction. (e) Section profile of the AFM picture showing the atomic roughness of mica substrate.

voltage 1 V. The scan rate of 1 Hz and the resolution of 256 pixels were selected for good quality imaging and moderate scanning time for an image.

3. Results and Discussions

The nanodroplets show radii ranging from 30 to 100 nm (Figure 1, panels a and b). A three-dimensional AFM image demonstrates that nanodroplets have a height between 1 and 25 nm (Figure 1c). The profile of the nanodroplets can be fitted by a spherical cap (Figure 1d). The AFM result also shows that the mica substrate displays the atomic roughness (Figure 1e).

Young's equation[2−5] and the modified Young's equation[6−9] are,

$$\sigma_{sv} - \sigma_{sl} - \sigma_{lv}\cos\theta_M = 0 \quad (1)$$

$$\sigma_{sv} - \sigma_{sl} - \sigma_{lv}\cos\theta = \frac{\tau}{r} \quad (2)$$

respectively, where σ_{sv}, σ_{sl}, and σ_{lv} are the surface tensions of the solid−vapor, solid−liquid, and liquid−vapor interfaces, respectively, θ_M is the macroscopic contact angle of the droplet, τ is the line tension, r is the droplet radius, and θ is the contact angle. The macroscopic contact angle was measured at room temperature in air by Contact Angle Measurement OCA20 (Dataphysics Instruments Gmbh, Filderstadt, Germany): θ_M for glycerol on mica is 24.5°. As shown in Figure 2a, for droplets with a radius of dozens of nanometers, quite a few different contact angles can correspond to a certain radius r, and vice versa, showing obvious contact angle hysteresis. The contact

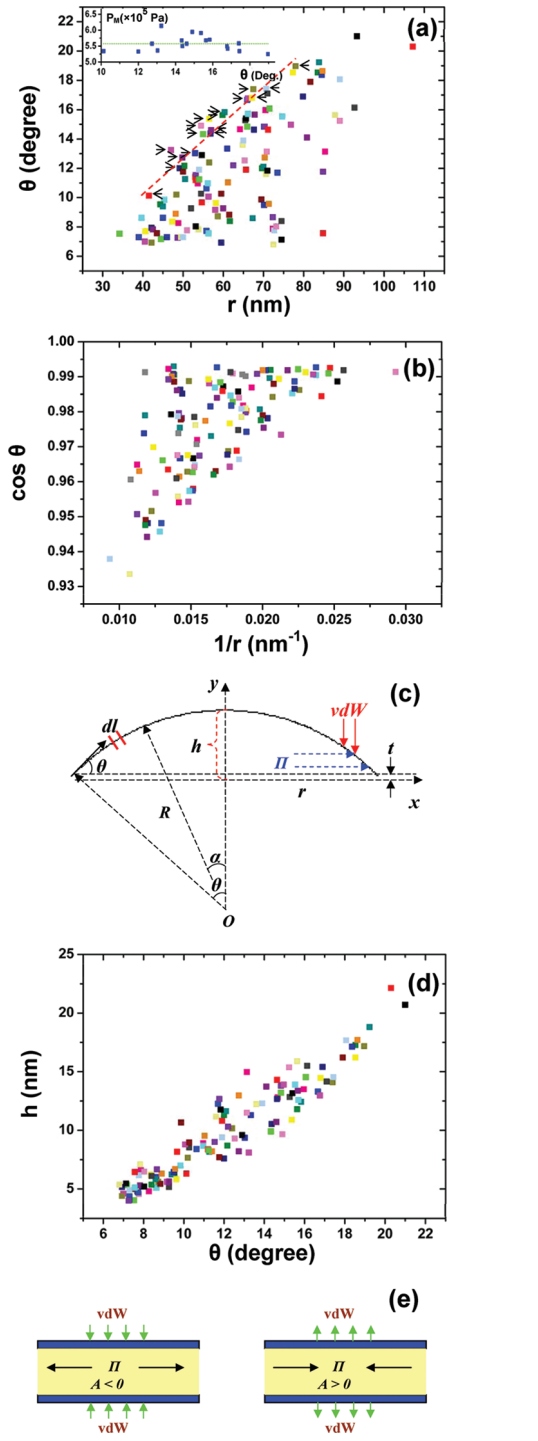

Figure 2. (a) A single contact angle θ corresponding to many radius values r, and vice versa. Inset: Threshold values of the inner pressure P_M in nanodroplets corresponding to different contact angles. The green line represents the median value. The error limit of the contact angle is ≤1°. (b) Scatter plot of cos θ versus 1/r displaying a nonlinear relationship for nanodroplets. The pattern of data constitutes a triangle shape. (c) Geometry illustration of a droplet. (d) The nanodroplet height h increasing with increasing contact angles. The colors chosen for representing the data in panels a, b and d are random. (e) Illustration of vdW force and disjoining pressure Π.

angles fluctuate over a wide range, approximately from 7° to 19°, which are obviously less than the macroscopic contact angle θ_M. Figure 2b shows that a scatter plot of cos θ versus 1/r yields a triangle shape rather than a linear function of 1/r. As cos θ

increases, we see a greater number of $1/r$ values. On the other hand, as $1/r$ decreases, an increasing number of cos θ can be seen.

There appears to be a maximum contact angle for each radius, or a smallest radius for a given contact angle (indicated by arrows in Figure 2a), with these approximately fitting a linear relationship (red dashed line). The pressure values calculated from the Laplace formula, $P_M = 2\gamma/R = 2\gamma \sin \theta/r$ (Figure 2c), for these nanodroplets are nearly equal (Figure 2a, inset), with some fluctuations near the median value 5.58×10^5 Pa (green line). On the basis of the Laplace formula, it is evident that smaller droplets have higher inner pressure. de Gennes et al. reported that very small droplets are thermodynamically unstable because of overpressure, thus they vanish in favor of larger droplets.[16] From our data, we have not seen the formation of a droplet whose inner pressure is larger than P_M, i.e., P_M is the threshold of the maximum pressure for stable nanodroplets, which is consistent with the assertion of de Gennes et al.

Due to the drop in nanoscale, the gravity effect can be neglected. The height of nanodroplets (Figure 2d) tends to increase with increasing contact angle, which is consistent with refs 11 and 14. The height of most droplets is less than 20 nm, in which the vdW force plays a crucial role.

When two parallel planar media are separated by distance D in another liquid medium, vdW force interaction between two media produces disjoining pressure in the liquid,[2,13]

$$\Pi = \frac{A}{6\pi D^3} \tag{3}$$

where A is the Hamaker constant. The vdW force can be attractive or repulsive, which corresponds to the retractive or repulsive disjoining pressure (Figure 2e) tending to thicken or thin the liquid thickness, respectively.

A transition zone with hyperbolic profile locates between the three-phase contact line and spherical cap of a drop,[15] which is illustrated in the inset of Figure 3a. Line tension was theoretically drawn out by the calculation of vdW interaction in the transition zone.[17−19] However, this analysis method is broken down for nanodroplet in this work, due to its whole spherical cap being able to be laid into this transition zone (Figure 3a, inset). Considering the very small dimension, if the transition zone of nanodroplets in this work exists, its size is much smaller than that of refs 17−19, corresponding to much weaker vdW interaction. Therefore, this line tension concept is not taken into account in this study.

Here we use the force analysis method introduced by de Gennes.[2] de Gennes took the effect of disjoining pressure into account on the force balance on a liquid portion near the contact line.

Young's equation and the modified Young's equation describe the force balance on the point laying on the contact line of a relative larger drop. However, due to vdW forces acting on the spherical cap of the drop, to evaluate the force balance, we need to take the force on the whole nanodroplet into account. In terms of the Derjaguin approximation,[13,20] the dispersion force on the spherical surface of nanodroplet caused by disjoining pressure is,

$$F = \int \Pi \, ds \tag{4}$$

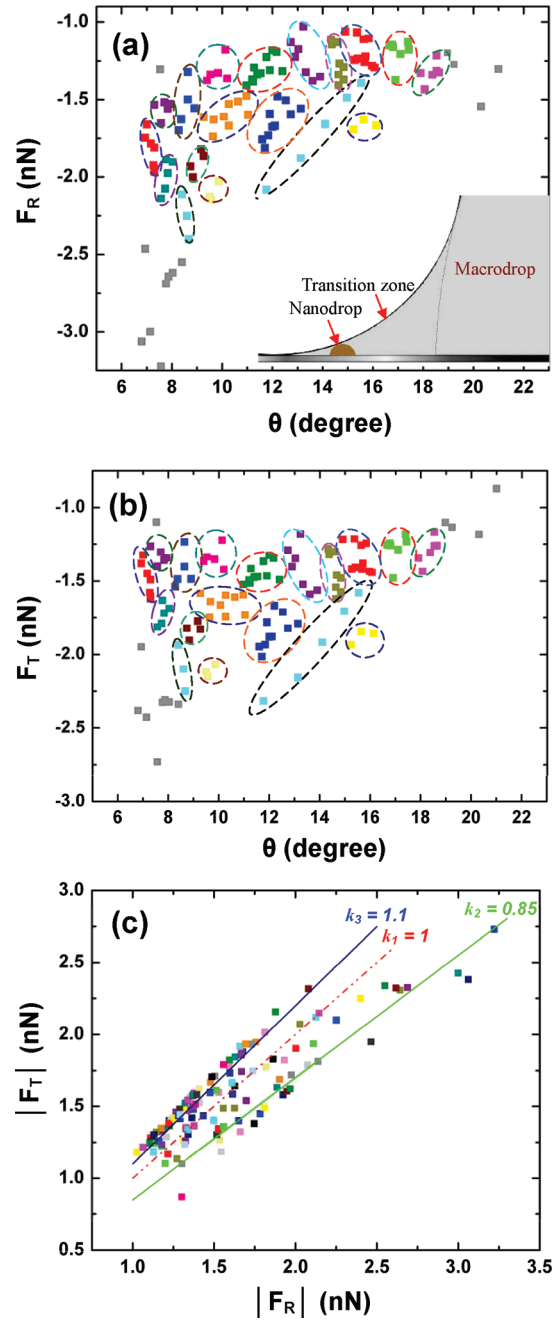

Figure 3. (a and b) Repulsive force F_R and resulting surface force F_T versus contact angle. We group the data by ellipses for which the patterns of F_T and F_R are similar. The same color in panels a and b represents the data for the same group. Inset in panel a: Transition zone. (c) Relationship between F_R and F_T, where k is the slope of the lines. The colors chosen for representing the data are random.

the integral element of spherical area $ds = 2\pi R \sin \alpha \, dl$, and the integral element of the circular arc length $dl = R \, d\alpha$ (Figure 2c). $F = \int_0^\theta [A/6\pi D^3] 2\pi R \sin \alpha R \, d\alpha$, and $D = R \cos \alpha - R \cos \theta + t$. α is the angle made by the y axis and the line connecting the sphere center O and sphere surface point, θ is the contact angle, R is the radius of the sphere fitting to the droplet profile, and t is the cutoff distance between the liquid surface and the substrate. Many researchers have proved the existence of a precursor film of one molecule in thickness ahead of the contact line,[21,22] thus t corresponds to one molecule thickness of glycerol, 0.6 nm.[23] After integrating the above equation, we obtain a repulsive dispersion force produced on the nanodroplets,

$$F_R = \frac{Ar}{6t^2 \sin\theta} \quad (5)$$

The Hamaker constant for two phases 1 and 2 interacting across a medium 3 is,[13]

$$A_{132} = \frac{3}{4}kT\left(\frac{\varepsilon_1 - \varepsilon_3}{\varepsilon_1 + \varepsilon_3}\right)\left(\frac{\varepsilon_2 - \varepsilon_3}{\varepsilon_2 + \varepsilon_3}\right) + \frac{3h\nu_e}{8\sqrt{2}} \frac{(n_1^2 - n_3^2)(n_2^2 - n_3^2)}{(n_1^2 + n_3^2)^{1/2}(n_2^2 + n_3^2)^{1/2}\{(n_1^2 + n_3^2)^{1/2} + (n_2^2 + n_3^2)^{1/2}\}} \quad (6)$$

where k is Boltzmann's constant, ε is the dielectric constant, T is the absolute temperature, h is Planck's constant, n is the refractive index, and ν_e is the absorption frequency. From the equation above, Israelachvili pointed out that as the dielectric properties (n^2) of the medium (glycerol, $n_3 = 1.472$) are intermediate between those of the two interacting media (N_2, $n_1 = 1$; and mica, $n_2 = 1.576$), the Hamaker constant is negative and the vdW force interaction between two media (N_2 and mica) results in the repulsive disjoining pressure across the medium (glycerol).[13] The Hamaker constant in the present work is -1.08×10^{-20} J. The dispersion force produced by this disjoining pressure tends to make the glycerol spread on the mica. Young's equation describes the mechanical balance of liquid droplets at macroscales for which the effect of vdW forces is negligible. For our experimental system, the droplets are at nanoscales, and the vdW forces should be included in the force analysis. Considering the force balance on the whole nanodroplet, the surface force acting on the perimeter of contact line is,

$$F_T = 2\pi r(\sigma_{sv} - \sigma_{sl} - \sigma_{lv}\cos\theta) = 2\pi r\sigma_{lv}(\cos\theta_M - \cos\theta) \quad (7)$$

Here we denote F_T as the resulting surface force. The value of θ_M measured in our work is 24.5°, which is close to the value of 23.5° reported in the ref 24. $F_T < 0$ indicates that it makes the nanodroplet contract, whereas F_R tends to spread the droplet. Thus the effects of F_R and F_T on droplet are opposite. F_T results from the contact angle θ being smaller than θ_M, which needs to be counteracted by F_R to reach the force equilibrium. The effect of vdW force on the contact angle is obvious: the contact angle can be as low as 7° (Figure 2a), far less than θ_M, and continuingly changes from 7° to 19°.

Panels a and b of Figure 3 show values of F_R and F_T calculated according to eqs 5 and 7, using the same data in Figure 2a. Most F_R and F_T values fall in the range from -2.0×10^{-9} to -1.0×10^{-9} N, showing F_R and F_T are of similar magnitude. For the same contact angle θ, the fluctuation of F_R and F_T values results from the different radius, indicated by eqs 5 and 7 as well. Surprisingly, the data points representing F_R and F_T (F_R and its corresponding F_T shown by the same color) in panels a and b of Figure 3 constitute similar patterns bound by ellipses. These similar patterns reveal that the variation of θ within a certain range leads to similar changes in F_R and F_T values. As indicated by eqs 5 and 7, both absolute values of F_R and F_T increase with decreasing contact angle and increasing radius, and decrease with increasing contact angle and decreasing radius. The ratio F_T/F_R is independent of the radius, but determined by the contact angle. Furthermore, we found that the ratio F_T/F_R varies between 0.85 and 1.1 (Figure 3c), indicating the magnitude of F_R and F_T is close even on the nanonewton scale.

As indicated by the Brochard-Wyart et al. study, the spreading force of liquid on the substrate caused by short-range interactions can be neglected in the case of Hamaker constant $A < 0$,[15] the same case as the present study. The microscopic roughness of mica in our experiments is at the atomic level. Thus, the contact angle hysteresis is unlikely due to the surface roughness of the substrate. The surface was exposed to air in a clean room for less than 30 s before a macrodroplet was blown by a gas jet. The adsorption of the air molecule to the substrate surface is believed to be the major source of the contact angle hysteresis. As the system is at equilibrium, the chemical force induced by air molecule adsorption balances the small force discrepancy between F_R and F_T, causing contact angle hysteresis. In the work of Checco et al.,[10] the heights of the droplets are much larger than that of the present work, thus the effect of vdW forces on the spherical cap of these drop can be neglected due to the retard effect. This may be the reason that there has been no obvious contact angle hysteresis observed. If no vdW forces exist, to produce contact angle hysteresis of the present nanodroplets, the extra force needs to reach about 10^{-9} N to balance F_T. Under vdW forces, this extra force reduces to $\Delta F = F_R - F_T$, which is on the order of magnitude of 10^{-10} N. Thus the force threshold of producing contact angle hysteresis is lowered significantly, for 1 order of magnitude. This force threshold can be more easily achieved by chemical heterogeneity, such as the adsorptions of chemical molecules on the mica substance.

On the other hand, Gaydos and Neumann[25] studied the contact angle hysteresis at macroscales and pointed out that the critical size of the chemical patch on a substrate for producing contact angle hysteresis is about 1 μm. As indicated by the above analysis, under the influence of vdW forces, contact angle hysteresis can more easily occur for nanodroplets, i.e., the hysteresis can be produced by much less chemical substance than that in macroscopic cases. The mechanism revealed in the present work has much meaning for varied morphology of soft matter on nanoscale, especially the contact angle of the adhesion of virus and organelle, in which different biological molecules can provide extra energy for contact angle hysteresis.

4. Conclusions

In summary, in this paper we have reported the contact angle hysteresis of nanodroplets on the substrate with atomic level roughness. We have proposed a mechanism that successfully accounts for the experimental observations: the change in the resulting surface force with varying contact angle and radius is almost completely counteracted by a repulsive dispersion force resulting from vdW forces, which significantly reduces the force threshold needed to produce contact angle hysteresis.

Acknowledgment. This project is supported by th National Natural Science Foundation of China (NSFC) and the National 973 Projects of China (No. 2002CB613505, MOST). J.M. is sponsored by SRF for ROCS, SEM. D.P.Y. is supported by the Cheung Kong Scholar Program, Ministry of Education, People's Republic of China. S.C. is supported by US NSF-CMMI 0649910 and by Project Nos. 10402001 and 10532010 from the National Natural Science Foundation of China (NSFC). We thank M. Robbins for discussions.

References and Notes

(1) de Gennes, P.; Badoz, G. J. translated by Reisinger, A. *Fragile Objects: Soft Matter, Hard Science, and the Thrill of Discovery*; Copernicus: New York, 1996.

(2) de Gennes, P. *Rev. Mod. Phys.* **1985**, *57*, 827–863.

(3) Shanahan, M. E. R. *J. Phys. D* **1987**, *20*, 945–950.

(4) Rowlinson, J. S.; Widom, B. *Molecular Theory of Capillarity*; Clarendon Press: Oxford, UK, 1982.

(5) Joanny, J. F.; de Gennes, P. *J. Chem. Phys.* **1984**, *81*, 552–562.

(6) Boruvka, L.; Neumann, A. W. *J. Chem. Phys.* **1977**, *66*, 5464–5476.

(7) Amirfazli, A.; Kwok, D. Y.; Gaydos, J.; Neumann, A. W. *J. Colloid Interface Sci.* **1998**, *205*, 1–11.

(8) Li, D. *Colloids Surf. A* **1996**, *116*, 1–23.

(9) Pompe, T.; Herminghaus, S. *Phys. Rev. Lett.* **2000**, *85*, 1930–1933.

(10) Checco, A.; Guenoun, P.; Daillant, J. *Phys. Rev. Lett.* **2003**, *91*, 186101.

(11) Barberis, F.; Capurro, M. *J. Colloid Interface Sci.* **2008**, *326*, 201–210.

(12) Lv, C.; Yin, Y.; Zheng, Q. *J. Appl. Math. Mech. (Engl. Transl.)* **2008**, *29*, 1251–1262.

(13) Israelachvili, J. N. *Intermolecular and Surface Forces*; Academic Press: New York, 1991.

(14) Xu, L.; Salmeron, M. *J. Phys. Chem.* **1998**, *B 102*, 7210−7215.

(15) Brochard-Wyart, F.; Di Meglio, J. M.; Quéré, D.; de Gennes, P. G. *Langmuir* **1991**, *7*, 335–338.

(16) de Gennes, P. G.; Brochard-Wyart, F.; Quéré, D. Translated by Reisinger, A. *Capillarity and Wetting Phenomena: Drops, Bubbles, Pearls, Waves*; Springer-Verlag: Duesseldorf, Germany, 2004.

(17) Joanny, J. F.; de Gennes, P. G. *J. Colloid Interface Sci.* **1986**, *111*, 94–101.

(18) Solomentsev, Y.; White, L. R. *J. Colloid Interface Sci.* **1999**, *218*, 122–136.

(19) Amirfazlia, A.; Neumann, A. W. *Adv. Colloid Interface Sci.* **2004**, *110*, 121–141.

(20) Parsegian, V. A.; *Van der Waals Forces*; Cambridge University Press: Cambridge, UK, 2006.

(21) Heslot, F.; Fraysse, N.; Cazabat, A. M. *Nature (London)* **1989**, *338*, 640–642.

(22) Daillant, J.; Benattar, J. J.; Léger, L. *Phys. Rev. A* **1990**, *41*, 1963–1977.

(23) Baudry, J.; Charlaix, E. *Langmuir* **2001**, *17*, 5232–5236.

(24) Wu, W.; Zhuang, H.; Nancollas, G. H. *J. Biomed. Mater. Res.* **1997**, *35*, 93–99.

(25) Gaydos, J.; Neumann, A. W. *Adv. Colloid. Interface Sci.* **1994**, *49*, 197–248.

JP905350P